

See discussions, stats, and author profiles for this publication at: <https://www.researchgate.net/publication/222476867>

H₂O concentrations in primary melts from supra-subduction zones and mid-ocean ridges: Implications for H₂O storage and recycling in the mantle

Article in *Earth and Planetary Science Letters* · January 1996

DOI: 10.1016/0012-821X(95)00203-0

CITATIONS

451

READS

135

2 authors:



Alexander V Sobolev

Université Grenoble Alpes

261 PUBLICATIONS 10,323 CITATIONS

SEE PROFILE



Marc Chaussidon

CNRS

365 PUBLICATIONS 10,273 CITATIONS

SEE PROFILE

Some of the authors of this publication are also working on these related projects:



Constraining Evolution of the Earth: Synergy of Geochemistry and Geodynamics. [View project](#)



Constraining Evolution of the Earth: Synergy of Geochemistry and Geodynamics [View project](#)



ELSEVIER

Earth and Planetary Science Letters 137 (1996) 45–55

EPSL

H₂O concentrations in primary melts from supra-subduction zones and mid-ocean ridges: Implications for H₂O storage and recycling in the mantle

Alexander V. Sobolev^{a,*}, Marc Chaussidon^b^a Vernadsky Institute of Geochemistry, Russian Academy of Sciences, 19 Kosigin Street, Moscow, 117975, Russia^b Centre de Recherches Pétrographiques et Géochimiques (CRPG–CNRS), 15 rue Notre Dame des Pauvres, BP 20, 54501 Vandoeuvre-Lès-Nancy Cedex, France

Received 27 February 1995; revised 9 October 1995; accepted 19 October 1995

Abstract

A total of 145 inclusions, trapped and isolated in Mg-rich olivine phenocrysts (Fo_{0.87–0.94}) from basalts and ultramafic lavas, and representing the most primitive mantle melts known, have been analysed by ion microprobe for their H₂O contents. This approach allows us to conduct a general survey of the distribution of water in primary melts derived from the mantle beneath mid-ocean ridges and above subduction zones. The primitive melts included in MORB olivines have low H₂O contents (mean at 0.12 wt% for N-MORB (14 samples), 0.17 wt% for T-MORB (9 samples) and 0.51 wt% for E-MORB (14 samples)). A strong decoupling between H₂O and K₂O has been found in some MORB primary melts which might well be explained by the presence of a H₂O-bearing CO₂-rich fluid. In contrast with mid-ocean ridges, primitive melts of subduction zones basalts are very rich in H₂O (between 1.0 and 2.9 wt% (mean at 1.7 wt%, 84 samples) for boninites and between 1.2 and 2.5 wt% (mean at 1.6 wt%, 24 samples) for island arc tholeiites). In addition, most of these melts have high H₂O/K₂O ratios which are consistent with a transfer of H₂O as a fluid phase from the subducted slab to the mantle wedge. For boninites and island arc primary melts, the present H₂O contents are $\approx 2.5 \times$ higher than commonly assumed, which suggests that the amount of H₂O released to the surface in arc magmatism has been previously underestimated.

1. Introduction

Because of its dramatic influence on the melting and the physical properties of mantle rocks [1,2], the presence of water in the mantle, either as H₂O molecules or OH⁻ groups, has been the subject of long term interest in geochemistry and geophysics. However, its concentration is difficult to determine

because mantle-related rocks, which are exposed at the surface, have commonly suffered several magmatic and post-magmatic processes which can readily alter their original water contents. Available estimates are based either on reconstruction of bulk contents of peridotite xenoliths from modal proportions and water concentrations of each mineral [3] or on analysis of mantle melts and reconstruction of the water content of the source [4–6]. Almost all data for H₂O contents of mantle-derived melts come from analyses of submarine glasses [7–13]. These glasses, even if optically perfectly fresh, may have lost part

* A.V.S.: Fax: 7-095-9382054; e-mail: asobolev@glas.apc.org.
M.C.: Fax: 33-83 51 17 98; E-mail: chocho@crpg.cnrs-nancy.fr

of their water by degassing at low pressures, as shown by the presence of abundant vesicles [7], or have gained exotic water by assimilation or contamination at a late stage, as shown by the correlations observed in some cases between water contents, δD and/or $\delta^{18}O$ values [13–15]. Additionally, nearly all the H_2O contents known for mantle melts might have been significantly increased by fractional processes since H_2O is incompatible in common crystalline phases. In fact, only three of all the MORB glasses analyzed for H_2O [4,6] and none from subduction zones fit the widely accepted criteria for primary mantle-derived melts (Mg number > 0.68 [16]).

The aim of this study was to determine directly by ion probe analysis the H_2O contents of the most primitive mantle melts known. These melts were trapped and isolated as melt inclusions of 40–200 μm in size in early olivine phenocrysts at the very beginning of crystallization. The olivines selected ($Fo_{0.87-0.94}$) are more Mg-rich than any previously investigated for the H_2O concentration of their inclusions [17–20] and hence are more representative of primary mantle melts. These olivines are commonly not at equilibrium with matrix glass but show euhedral shapes and primary melt inclusions so that they can be considered as early intratelluric phases or xenocrysts which originated in the same plumbing system. Additionally, H_2O concentrations were measured in melt inclusions trapped in olivine microphe-nocrysts and in matrix glasses in order to characterize the possible loss and/or gain of water during the evolution of mantle melts. Different localities and geodynamic environments of oceanic lithosphere were studied.

Although leakage of water through the surrounding olivine by volume diffusion of H or of H_2O molecules could occur [21,22] the H_2O contents of melt inclusions are believed to be better estimates of primary H_2O contents than those of the matrix glasses, because the latter act as a completely open system for volatiles when saturated by a fluid phase. Despite the high diffusion rates recently found for H in olivine [21] some of the present melt inclusions have very high H_2O contents of up to $\approx 4.4wt\%$. Modelling of diffusive re-equilibration of melt inclusions in phenocrysts with matrix glass has shown that the process is much more rapid and more effi-

cient if the element considered is compatible or just moderately incompatible [22]. However, the present inclusions show high disequilibrium (see Fig. 2) for both H_2O which is strongly incompatible in olivine [3], and for Mg–Fe which are compatible in olivine. This implies that even if the H_2O contents of the melt inclusions represent a minimum H_2O content for the primary melts, the effect of re-equilibration of the trapped melts with matrix melts by diffusion through the olivine host was in most cases minimal.

2. Sample selection and inclusion treatment

The samples studied, either glasses or coarse crystalline rocks, were selected on the basis of (1) the high Mg content of olivine (between Fo 87 and Fo 94 mol%) which indicates crystallization from nearly primary magmas of mantle origin [16] and of (2) the presence of primary melt inclusions trapped during crystal growth [23] with no evidence of decrepitation (small shrinkage bubbles (less than 5 vol%) and no visible cracks). All the glasses contain abundant vesicles, showing fluid saturation during quenching. Olivine phenocrysts (typically 0.5–10 mm in size) and microphe-nocrysts (typically 0.1–0.5 mm in size) were studied in the same samples for the composition and petrography of the melt inclusions. In glassy samples, melt inclusions in olivines commonly consist of glass with or without shrinkage bubbles. In coarse crystalline samples, most inclusions in olivines comprise skeletal quenched clinopyroxene crystals, opaque phases, glass, and shrinkage bubbles.

The naturally quenched glassy melt inclusions were studied unheated. However, they are usually not in equilibrium with the host olivine as shown by Mg–Fe partitioning criteria [24], which indicate significant olivine crystallization on the walls of the cavity [23,25,26]. Therefore, corrections were applied to the measured compositions to take into account the effect of olivine growth on the walls of the inclusions. The details of this correction procedure have already been described [27,28] and will therefore not be given here. It suffices to say that the principle of the correction is to reconstruct the composition of the trapped melt by modelling the reverse fractional crystallization of olivine up to the equilibrium of included melt with host olivine [25] at 1 atm

and $\text{Fe}^{2+}/\text{Fe}^{3+}$ ratios in the melt corresponding to the oxygen fugacity of the quartz–fayalite–magnetite buffer. Water is assumed to be totally incompatible in olivine. Uncertainties introduced by these corrections because of possible variations in oxygen fugacity or in post-entrapment Fe–Mg exchange between olivine and melt are small (i.e., less than 12% relative on the amount of added olivine for variations in the oxygen fugacity of ± 1 log unit around QFM). Additional corrections were applied for inclusions which show significant loss of Fe due to Fe–Mg exchange between the trapped melt and the host olivine after entrapment (see [27] for details). Such cases are quite evident from inclusions which have lower FeO contents than that of primitive rocks and glasses from the same suite which always have a restricted range of FeO contents ($\pm 10\%$ relative). The effect of all these corrections on the H_2O content of the inclusions is less than 20% relative for 90% of the inclusions studied.

In contrast with naturally quenched glassy melt inclusions, the partly crystallized melt inclusions in olivines were heated up to the temperature of dissolution of the last silicate crystal in the cavity or total homogenization and quenched [23]. This procedure can lead to the loss of some H_2O from the inclusions because of the fast diffusion of H through the volume of host olivine in the presence of the strong pressure gradient of H between the inclusion and the external atmosphere [27]. To minimize this effect the total time of exposure at a temperature of more than 1000°C was reduced to less than 15 min. However, even for such short durations up to 30% of the original H_2O can be lost from the inclusions (our unpublished data on the Kluchevskoy volcano). Thus, the H_2O contents measured in heated inclusions must be considered as minimum estimates of the original concentration. In a second step, the compositions of the melt inclusions quenched from the temperature of the last cotectic phase dissolution were corrected for the potential crystallization of olivine in the same way as for unheated inclusions. The composition of the totally homogenized melt inclusions represents the original composition of the trapped melt [23] unless the inclusion was significantly overheated due to the decomposition of H_2O [27]. Overheated inclusions were rejected using the criteria for equilibria between olivine and melt.

3. Analytical techniques

The H_2O contents in the glasses were measured with a Cameca IMS 3f ion probe at the CRPG–CNRS (Nancy, France). The samples were polished to $1\ \mu\text{m}$, ultrasonically cleaned in pure alcohol, baked at 40°C overnight, coated with gold, and kept at 40°C until introduction into the ion probe. The intensities on peaks $^1\text{H}^+$ and $^{30}\text{Si}^+$ were recorded, under bombardment of an O^- primary beam with an intensity of 10–15 nA and a size of $\approx 10\ \mu\text{m}$, at a mass resolution of 1200 and with an energy filtering of $-100 \pm 10\ \text{V}$. In order to minimize the H_2O background, the ion probe was repeatedly baked at 120°C overnight, and a liquid nitrogen cold trap in the source was used [29]. Measurements were then started when the $^1\text{H}^+ / ^{30}\text{Si}^+$ ratio measured on the olivine hosts was lower than a value corresponding to a H_2O content of 0.03 wt%. The olivines being supposed to contain water at the ppm level only, this value of 0.03 wt% H_2O is thus the estimate of the detection limit of water by ion probe under these conditions. The measured $^1\text{H}^+ / ^{30}\text{Si}^+$ ratios were calibrated versus the wt% $\text{H}_2\text{O}/\text{wt}\%$ SiO_2 ratios in the range 0.09–8 wt% H_2O (Fig. 1) using seven glass standards of water contents analyzed at the

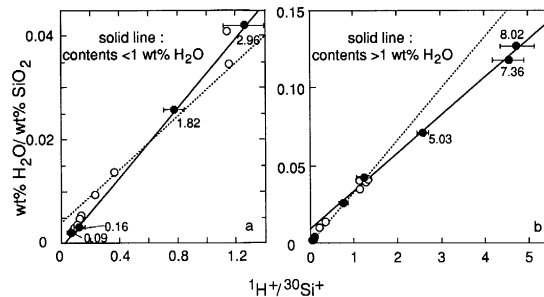


Fig. 1. Calibration curves for H_2O concentration measurements by ion microprobe. Two slightly different curves (see text) were used for contents of < 1 wt% H_2O (a, $\text{wt}\% \text{H}_2\text{O}/\text{wt}\% \text{SiO}_2 = 0.0332716 \times ^1\text{H}/^{30}\text{Si} - 0.000329$) and contents of > 1 wt% H_2O (b, $\text{wt}\% \text{H}_2\text{O}/\text{wt}\% \text{SiO}_2 = 0.025757 \times ^1\text{H}/^{30}\text{Si} + 0.003940$). ● = CRPG standards used to determine the calibration curves. The error bars indicate the reproducibility for these standards, which varies between 2% relative (2σ) and 16% relative (2σ), the counting statistics being always better than 5% relative. Also shown for comparison are other glasses measured by the Fourier transform infrared technique, high-temperature gas chromatography and mass spectroscopy ([33] and unpublished data).

CRPG by heating under vacuum, conversion of H₂O to H₂ in a uranium furnace, and manometric measurement, the procedure commonly used for isotopic measurement of H₂. This calibration curve was checked by analysis of eleven additional glasses which covered the entire compositional range of the inclusions and which were analyzed by either the Fourier transform infrared technique, high-temperature gas chromatography or mass spectrometry (Fig. 1). It was found that the use of two separate calibration curves (Fig. 1), one for low water contents and another for high water contents, gives a better fit for the standards. This feature, which was not noted in previous studies, suggests that the emissivity of H⁺ is slightly higher for high water contents than for low water contents. This is not yet theoretically understood but it could be related to the observed change of speciation of water in glasses that contain

a higher proportion of molecular H₂O to hydroxyl groups at high H₂O contents than at low H₂O contents [30]. Because our two calibration curves crosscut at ≈ 1 wt% water it was decided for simplicity to use one curve for contents lower than 1 wt% H₂O and the other for contents higher than 1 wt% H₂O (Fig. 1). No strong matrix effects were found on our standards ranging in SiO₂ content between ≈ 49 and ≈ 71 wt% (a larger range than that of the melt inclusions), probably because a strong energy filtering of -100 ± 10 V was used. This is known to decrease matrix effects (e.g., [31]). The reproducibility of the analyses for ten measurements made over a 5 day interval was 8% relative (2σ) for one of the samples with the highest water content (3.2 wt% H₂O) and 11% relative (2σ) for one sample with low water contents (0.4 wt% H₂O). Counting times on the ¹H⁺ peak were varied so that

Table 1
H₂O and selected major element contents of representative melt inclusions from mid-ocean ridge and supra-subduction zones

	Melt inclusion treatment*	Melt inclusion					Host olivine		Melt inclusion corrected					Matrix glass				
		Al ₂ O ₃	FeO	MgO	K ₂ O	H ₂ O	Fo #	Ol cor	Al ₂ O ₃	FeO	MgO	K ₂ O	H ₂ O	Al ₂ O ₃	FeO	MgO	K ₂ O	H ₂ O
<i>N-MORB</i>																		
20-5/82 (Siqueiros F.Z., EPR)	U	18.03	7.31	9.11	0.02	0.13	0.910	0.032	17.32	7.33	10.37	0.02	0.12	17.26	8.03	9.54	0.05	0.11
20-5/89 (Siqueiros F.Z., EPR)	U	17.97	7.79	9.18	0.03	0.10	0.903	0.030	17.34	7.83	10.35	0.03	0.10	17.26	8.03	9.54	0.05	0.11
84-10/135A (12°N, MAR)	U	17.92	8.95	10.01	0.03	0.12	0.895	0.037	17.24	9.01	11.44	0.03	0.12	17.83	8.76	9.72	0.03	0.13
<i>T-MORB</i>																		
DR8CH31-344 (Famous)	U	16.81	7.25	6.23	0.02	0.20	0.899	0.108	15.07	7.82	10.73	0.02	0.18	15.99	7.08	8.88	0.04	0.16
DR8CH31-344 (Famous)	U	17.40	7.38	5.72	0.17	0.17	0.904	0.136	15.11	8.01	11.40	0.15	0.15	15.99	7.08	8.88	0.04	0.16
<i>E-MORB</i>																		
30-1L/8 (14°N, MAR)	U	16.32	6.1	7.01	0.07	0.63	0.909	0.038	15.87	6.17	9.02	0.07	0.60	15.21	10.07	6.00	0.57	0.60
30-1L/31A (14°N, MAR)	U	16.86	6.09	6.65	0.40	0.62	0.906	0.059	15.90	6.36	9.15	0.38	0.58	15.21	10.07	6.00	0.57	0.60
8-13-36 (15°N, MAR)	H	15.37	6.43	10.72	0.03	0.60	0.905	0	15.43	6.45	10.76	0.03	0.60	-	-	-	-	-
8-13-38 (15°N, MAR)	H	15.06	6.63	11.17	0.13	0.59	0.904	0	15.15	6.67	11.24	0.13	0.59	-	-	-	-	-
<i>High-Ca boninites</i>																		
Trd-39/29 (Cyprus)	H†	13.13	5.62	14.00	0.08	2.41	0.921	0.10	11.55	8.24	15.81	0.07	2.12	-	-	-	-	-
Trd-41/41 (Cyprus)	H†	13.26	5.77	14.99	0.16	2.15	0.926	0.10	11.80	8.33	16.72	0.15	1.90	-	-	-	-	-
Trd-41/glic (Cyprus)	U†	14.45	5.76	3.58	0.01	1.90	0.910	0.27	10.87	8.60	14.39	0.01	1.38	-	-	-	-	-
3-47/13b (Tonga trench, Pacific)	U†	12.75	6.57	4.38	0.50	3.19	0.920	0.26	9.58	7.97	15.39	0.37	2.36	-	-	-	-	-
5-25-3 (Tonga trench, Pacific)	U	11.64	6.55	7.23	0.13	3.50	0.940	0.41	7.06	9.11	23.40	0.08	2.03	13.11	10.01	5.83	0.20	1.00
77/28-44 (Hunter FZ, Pacific)	U†	11.58	6.26	8.89	0.19	3.11	0.911	0.07	10.86	6.52	11.67	0.18	2.90	13.63	8.43	6.95	0.20	1.70
AAV-7-103 (Bonin isl., Pacific)	U	15.33	4.69	3.43	0.44	2.50	0.904	0.26	11.35	8.49	13.57	0.32	1.81	-	-	-	-	-
<i>Low-Ca boninites</i>																		
41F/OL (Cape Vogel, Papua New Guinea)	U†	9.91	0.82	0.84	0.13	2.85	0.940	0.56	4.44	8.36	25.49	0.06	1.25	-	-	-	-	-
173 (New Caledonia)	U†	13.01	3.60	7.60	0.51	4.40	0.934	0.33	8.71	7.84	19.63	0.34	2.86	-	-	-	-	-
<i>Island arc tholeiites</i>																		
Trd-150 (Troodos, Cyprus isl.)	H†	15.67	6.29	12.64	0.01	1.70	0.909	-0.04	16.14	6.83	10.52	0.01	1.75	-	-	-	-	-
Trd-150-28 (Troodos, Cyprus isl.)	H†	14.21	6.51	11.77	0.03	1.76	0.900	-0.04	14.88	6.93	9.78	0.03	1.81	-	-	-	-	-
Trd-150 Ol 168 (Troodos, Cyprus isl.)	H†	16.45	5.98	9.00	0.37	1.43	0.896	0.03	15.94	7.13	9.75	0.36	1.36	-	-	-	-	-
101/1-13 (Hunter FZ, Pacific)	U†	16.62	6.65	6.21	0.21	2.21	0.886	0.05	15.96	7.02	8.35	0.21	2.09	16.40	8.02	5.18	0.29	1.33
04-1 (Kamchatka)	H	14.55	7.12	8.18	0.59	1.97	0.897	0.06	13.92	8.32	10.31	0.56	1.85	17.25	8.94	4.64	1.16	0.10
4-2a (Kamchatka)	H†	16.49	7.33	7.70	0.79	2.58	0.873	0.05	15.58	8.52	8.75	0.74	2.46	17.25	8.94	4.64	1.16	0.10

Major elements were analyzed using routine electron microprobe procedure (e.g., [34]), with the exception of the low K₂O contents in glasses (< 0.1 wt%). The latter were reanalyzed with increased counting time (30 s on three points) to obtain an accuracy of 0.015 wt% (2σ) for K₂O.

* U = inclusions studied unheated; H = inclusions heated for homogenization (see text).

† These inclusions were also corrected for post-trapping Fe–Mg exchange (see text).

Ol cor = amount of olivine that crystallized on the walls and used for the correction of the composition of the melt inclusion (see text).

for all samples the counting statistics were better than $\pm 5\%$ relative. Taking into account the main source of uncertainty—the calibration curve—the accuracy obtained on the H_2O contents is estimated to be always better than $\pm 20\%$ over the entire range investigated, even if many of the measurements are more precise.

4. Results

Major element and water contents are given for a set of representative samples in Table 1 for mid-ocean ridges (classically divided on the basis of incompatible element contents into normal basalts [N-MORB], transitional basalts [T-MORB] and enriched basalts [E-MORB]) and for supra-subduction zones (SSZ). The complete dataset is available on request from the authors. The SSZ lavas are represented by high-Mg basalts (HMB) from the world's most active island arc volcano (Kluchevskoy, Kamchatka), which are parental to typical island arc high-alumina

basalts [32], by island arc tholeiites (IAT) from the Hunter fracture zone and from the lower pillow lava section of the Troodos ophiolite [33], and by boninites (BON) from Troodos, Cape Vogel, Tongan, the Hunter fracture zone and New Caledonia.

4.1. First-order observations: High H_2O contents of SSZ primary melts

The melt inclusions have MgO contents ranging between 7.3 and 25.5 wt%, which clearly demonstrate that most of them correspond to the most primitive melts known for supra-subduction and oceanic environments. The highest MgO concentrations were found in boninitic primary melts and are consistent with independent estimates made from the composition of glasses and whole rocks which give ≈ 20 wt% for Cape Vogel boninite [34], 17–24 wt% for Tongan boninites [26,27] and 19–22 wt% for Troodos boninites [33]. The water contents of the primitive melts from boninites range between 1.0 and 2.9 wt% (84 samples, mean at 1.7 wt%) and

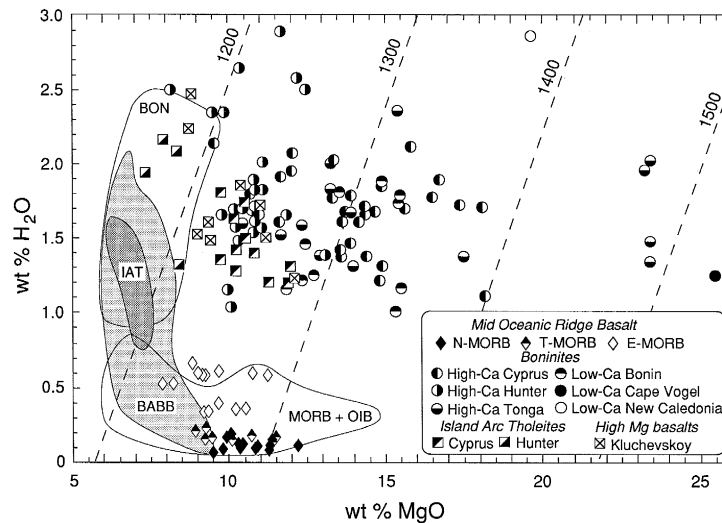


Fig. 2. H_2O vs. MgO contents of primary melt inclusions. The fields correspond to glasses containing more than 6 wt% MgO from similar geodynamic environments [4–15]. Isotherms for the melts (between 1200 and 1500°C, dashed lines) were calculated for a pressure of 10 kbar using the following equation: $T^{\circ}C = 1042 + 18.79 \times MgO - 33.1 \times H_2O + 5 \times P$, where MgO and H_2O concentrations in the melt are in wt% and P is in kbar. This equation is a combination of the empirical equation for the dependence of liquidus temperature on the MgO content of the melt [36] and of the experimental equation for the effect of H_2O on liquidus temperature [37]. With respect to MgO his equation is valid for most of the MgO range of the present inclusions (10–25 wt% MgO [36]), but the fact that the effect of H_2O for high MgO melts is poorly known could add some uncertainty to the temperature estimates. Note that the high H_2O contents of the melt inclusions are for unfractionated melts (high MgO); these water contents are much higher than most of those that can be calculated for primary melts from the basalt glasses which have suffered significant fractionation (see text).

those of island arc tholeiites range between 1.2 and 2.5 wt% (24 samples, mean at 1.6 wt%). These contents are at first glance roughly similar to the previous data on evolved melts [8,12–14,35], but are in fact $1.5\text{--}3\times$ higher than what can be expected in the parental melts of these evolved melts (Fig. 2). This is in particular true for boninites, while for island arc tholeiites very high water contents (between 3 and 6 wt% H_2O) were previously reported for melt inclusions in olivine from the high-Al basalts of Fuego volcano, Guatemala [20]. Starting from our primary melt compositions, the water contents that can be extrapolated for evolved melts comparable to those previously published are also very high. For instance, a content of at least 3.5–4.0 wt% H_2O is predicted for evolved high-Al basaltic and andesitic melts from the H_2O -rich primary melts of the Kluchevskoy volcano, after the 30–40% of fractional crystallization required to reach evolved compositions similar to those of Fuego volcano [20] or those of the matrix glasses (Table 1).

In contrast with the SSZ results, primitive melt included in MORB olivines has much lower water contents, at between 0.34 and 0.66 wt% for E-MORB (14 samples, mean at 0.51 wt%) and between 0.07 and 0.19 wt% for N-MORB (14 samples, mean at 0.12 wt%). The T-MORB fall in the range between N-MORB and E-MORB, with water contents between 0.13 and 0.23 wt% (9 samples, mean at 0.17 wt%).

4.2. Comparison between melt inclusions and matrix glasses

Systematic differences in H_2O contents between inclusions in olivine phenocrysts, inclusions in olivine microphenocrysts and matrix glasses are observed for all of the SSZ samples (Fig. 3a). This is not the case for MORB. For SSZ, the melts trapped in olivine phenocrysts tend to be significantly richer in H_2O than the late melts trapped in olivine microphenocrysts, which have contents similar to those

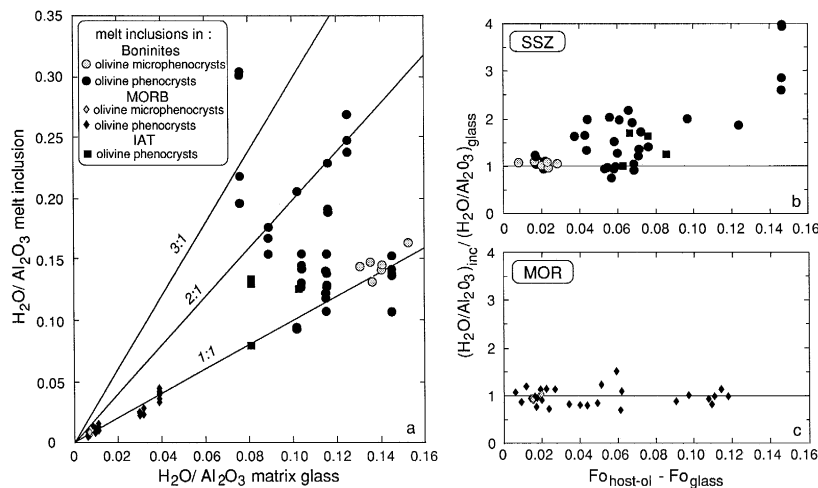


Fig. 3. Comparison of the H_2O contents of melt inclusions and matrix glasses. (a) $\text{H}_2\text{O}/\text{Al}_2\text{O}_3$ ratios of melt inclusions vs. those of matrix glasses. H_2O was normalized to Al_2O_3 for melt inclusions and glasses in order to exclude the possible effect of olivine and pyroxene crystallization, which will influence both concentrations but not the ratio of the concentrations. Melts included in olivine microphenocrysts are similar to matrix glasses for all environments, while for SSZ basalts melts included in olivine phenocrysts are up to $4\times$ more H_2O rich than matrix glasses. (b) and (c) Relative H_2O enrichment of inclusions compared to glasses (measured as $[(\text{H}_2\text{O}/\text{Al}_2\text{O}_3)_{\text{inclusion}} / (\text{H}_2\text{O}/\text{Al}_2\text{O}_3)_{\text{glass}}]$) vs. degree of disequilibrium of host mineral and matrix glass, presented as the difference between the measured composition of olivine and the composition of olivine calculated at equilibrium with host glass using the model of Ford et al. [49] for $\text{FeO}/\text{Fe}_2\text{O}_3$ in the melt of 8. The H_2O contents of the SSZ melts changed in the course of their evolution, as is evident from primary melt inclusions (the most ‘disequilibrated’ olivines being the richest in H_2O), in contrast to MORB melts which have constant H_2O contents.

of the latest melts represented by the matrix glasses. The most primitive melts are enriched in H_2O by a factor of 1–4, this being positively correlated with the degree of olivine disequilibrium with matrix glass (Fig. 3b). These data imply that the SSZ melts which are erupted at the sea bottom (most of the samples) or at the surface (Kamchatka HMB) have lost most of their initial H_2O (up to more than 96% for Kamchatka HMB). Degassing in the course of the evolution of the SSZ melts is the most likely process because (1) the glasses are saturated with a H_2O -rich fluid which is obvious from the presence of H_2O -bearing fluid inclusions in the glasses [27] and (2) the H_2O and MgO contents decrease together. In the case of MORB (Fig. 3c), no strong variation in the H_2O content of the melts is observed from their generation to their emplacement, which suggests that they were never saturated with a H_2O -rich fluid.

4.3. Second-order observation: Decoupling between H_2O and K_2O in MORB

In addition to the well-known correlation between H_2O and K_2O observed for MORB glasses [6,39], the present data also show that most of the primary or nearly primary melts follow the same relationship (Fig. 4), the lowest H_2O and K_2O contents being characteristic of N-MORB and the highest of E-MORB, with T-MORB in between. This correlation demonstrates the similar incompatible behaviour of K and H_2O with respect to common silicate minerals, albeit with a rather greater incompatible affinity of K [6,39]. What is completely new in our dataset is the presence in each MORB type of melts depleted in K but with relatively high H_2O contents. Such melts, which are ultradepleted in highly incompatible elements, have recently been shown to exist in different geodynamic settings [28,33]. The lack of any correlation between the K_2O and the H_2O contents is clear for the different melt inclusions of a given sample, and this for several samples of different compositions (Fig. 4). This decoupling of H_2O and K_2O in the highly depleted primary melts of MORB leads to anomalously high H_2O/K_2O ratios of more than 10, which have never before been reported for MORB glasses.

A simple explanation of this decoupling could be the buffering effect due to the presence of a H_2O -

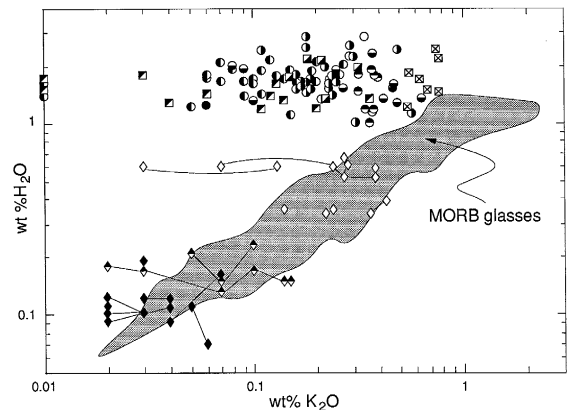


Fig. 4. H_2O vs. K_2O contents of primary melts (symbols are the same as in Fig. 2). For MORBs, inclusions in olivines coming from the same sample are joined by a line. Field derived for N-MORB and E-MORB from the study of oceanic basalt glasses [6,38] is shown for comparison. Although the agreement is good between MORB primary melts and MORB glasses, a significant decoupling of H_2O and K_2O is observed for several samples. For SSZ melts, a very strong decoupling of H_2O and K_2O is observed for most of the samples, suggesting the introduction of water as a fluid phase in the mantle wedge.

bearing and K-poor phase, such as a CO_2 -rich fluid. Dense CO_2 inclusions, indicating a magmatic pressure of CO_2 at around 1.5–2.5 kbar, have indeed been observed in high-Mg olivine phenocrysts from the same samples. Preliminary Raman studies of such inclusions in E-MORB (Sobolev and Dubessy, unpublished results) have shown H_2O concentrations of 3 mol% which correspond to a partial H_2O pressure of 40–50 bar and to 0.6–0.7 wt% H_2O in the equilibrium melt. Similar CO_2 -rich fluids with variable H_2O contents, that appear during deep degassing of MORB melts, could produce a permanent background at every location of active MORB volcanism and could buffer the H_2O concentration of small, separate melt fractions represented by ultradepleted melts [28]. The huge mass of MORB melts should not be affected by such a process because the total amount of CO_2 fluid expected is not more than ≈ 0.01 in mass of the melt. An alternative explanation for this decoupling between K_2O and H_2O in MORB could be the diffusion of external H_2O inside the inclusion to reach a concentration similar to that in the matrix melt. However, this scenario contradicts the fact that the olivine hosts of such inclusions

show no diffusional re-equilibration of Mg–Fe with the matrix glass, which should be expected to occur more rapidly than for H₂O, which is incompatible in olivine [22].

A similar decoupling of H₂O and K₂O is also present for SSZ magmas from Troodos, and can be explained by a buffering effect of a H₂O-rich fluid phase in the source of the SSZ magmas (see next section).

5. H₂O distribution in the sources of the primary melts

The H₂O concentrations in depleted MORB primary melts (in the range 0.07–0.16 wt%) correspond to 80–330 ppm in the mantle source for 10–20% aggregated fractional melting, or batch melting using a bulk K_d for H₂O of 0.01 [4,5]. Similarly, the H₂O content calculated for the mantle sources corresponding to the primary melts of either T-MORB type (\approx 0.17 wt% H₂O) or E-MORB type (0.34–0.60 wt% H₂O) are, respectively, 190–290 ppm and 200–950 ppm for 5–15% partial melting. These values are entirely consistent with previous estimates for the sources of N-MORB (100–180 ppm H₂O) and of E-MORB (250–450 ppm H₂O) [4], which were obtained from the study of submarine basaltic glasses. This consistency is also in agreement with the fact that the primary melt inclusions in olivine suggest no significant variation in the H₂O content of MORB type melts during their evolution. In contrast, degassing of H₂O is evident for the SSZ magmas (Fig. 3). Thus, the maximum values found for boninites (2–2.9 wt% H₂O) and for island arc tholeiites (2–2.5 wt% H₂O) are the most reasonable estimates for the initial H₂O contents in their primary melts. This implies that, in the case of more than 5% melting, the minimum H₂O concentration in the SSZ mantle sources is between 1190 and 1900 ppm.

The H₂O contents found for the source of N- and T-MORBs, and some of the H₂O contents for the source of E-MORB, are consistent with the amount of H₂O that can be contained in an anhydrous lherzolite (up to \approx 300 ppm H₂O [3]), this being probably a lower limit since olivine alone accommodates up to 300 ppm H₂O [40]. In contrast, the

source for the SSZ magmas must be different. Indeed, the minimum H₂O contents found for the upper mantle in subduction zones (from 1190 to 1900 ppm) far exceed the amount of H₂O that could be stored in common anhydrous mantle minerals and thus require the presence either of additional H₂O-bearing crystalline phases or of H₂O-rich melts or fluids. However, the temperatures indicated for the mantle sources of SSZ primary melts by the melt inclusions ($>$ 1200°C for 10 kbar, Fig. 2) are too high for common hydrous silicates (e.g., amphibole and phlogopite) to be stable in the mantle wedge, at least in the melt source area. It seems more likely that water was introduced in the mantle wedge as fluids or melts produced by the dehydration/melting of the hydrous silicates formed with increasing metamorphism in the subducted slab. As shown by recent experiments [41], the release behaviour of water from the subducted slab depends primarily on the pressure–temperature conditions and for certain conditions water can well ascend to regions of the mantle wedge which are above their wet solidus, thus causing melting.

6. The ‘boninite paradox’

It is clear from Fig. 2 that very high temperature melts ($>$ 1350°C) belong solely to the boninite family. Although these melts show high temperatures, they also show an enrichment in H₂O. At first glance these results contradict the well-known behaviour of water in decreasing the melting temperature of peridotite and thus could be referred to as the ‘boninite paradox’. This has already been discussed for boninites from different localities (e.g., [27,33]) but the present dataset shows that it is in fact a general feature of the boninites. The most simple explanation for this apparent paradox would be that boninites formed by the remelting of an extraordinary hot residual mantle which could be related to mantle plumes, the melting being driven by a flux of H₂O fluid from the subducted slab. One major point is that this residual mantle is too hot to be related to MORBs, as is commonly suggested for boninites (e.g., [42]), but that it is very close in temperature to mantle plumes [43]. The independent geochemical evidence for the involvement of plume components

in the origin of boninites [27,33] strongly supports this hypothesis.

7. H₂O cycling in subduction zones

The extremely high H₂O/K₂O ratios of some melt inclusions from Troodos (up to ≈ 200 , see Fig. 4) and the generally high H₂O/K₂O ratios of most of the boninite primary melts clearly demonstrates that, at variance with previous suggestions [42], the metasomatic component derived from the slab is not necessarily enriched in LILE. In addition, these high H₂O/K₂O ratios are very different from those of the subducted slab both before subduction ($\approx 1\text{--}4$ [44]) and after water removal in arc magmatism ($\approx 0.7\text{--}1$ [6]), which implies that water is not simply extracted from the subducted slab and transferred to the mantle wedge dissolved in a melt. This conclusion is of importance for the estimation of the geochemical fluxes between the mantle and the subducted slab [45]. The high H₂O/K₂O ratios of the present primary melts indicate that water was transferred by a process capable of decoupling two strongly incompatible elements such as K and H₂O, and most probably by a fluid phase [12,20]. This transfer of H₂O as a fluid phase is consistent with the high H₂O/K₂O ratios observed for high-pressure fluids [46] but cannot be demonstrated for all the present island arc samples because the Kluchevskoy primary melts have much lower H₂O/K₂O ratios. Finally, the high H₂O/K₂O ratios also imply that the mantle source of boninites is very poor in K₂O, which is consistent with its depletion during several episodes of partial melting [42].

Although evidence for the presence of subducted water in the upper mantle is provided by the high δD values (between -56 and -28‰) of some amphiboles from peridotite xenoliths from the Massif Central (France) [47], major uncertainties still exist concerning the behaviour of water in subduction zones [48] and concerning the amount of water which can be retained in metamorphic minerals within the subducted slab [2]. A precise quantification of the amount of H₂O introduced into the mantle by subduction is beyond the scope of this work, but important constraints are imposed by the

high water contents of primitive melt inclusions from IAT. If the Kluchevskoy data are representative of island arc lavas, and if the highest H₂O contents are the best estimates of the primary melt compositions, a value of at least 2.5 wt% H₂O is suggested for primary island arc melts. Such high water contents are consistent with recent experimental estimates [37] but are $2.5 \times$ higher than previously assumed for this type of magma [48]. This would increase the previous estimate for water recycling efficiency at subduction zones (ratio between water released in arc magmatism and the total water subducted) from $\approx 15\%$ to $\approx 40\%$. This leaves the possibility that most of the subducted H₂O is recycled back to the surface beneath island arcs, as previously suggested from the H₂O/He ratios of some arc and back arc lavas [49].

Acknowledgements

We are grateful to the following persons for donation of samples and prepared inclusions: W. Cameron (Cape Vogel boninite), J.F. Casey (Siqueiros fracture zone MORB), R. Clochiatti (FAMOUS MORB), L. Danyushevsky (Tonga, New Caledonia and Bonin Island boninites), T. Falloon (Tonga boninites), S. Hubunaya (Kamchatka HMB), V. Kamenetsky (Hunter zone boninites and IAT), R. Magakyan (Mamonia, Cyprus and Bonin Island boninites and Petrov fracture zone MORB), M. Portnyagin (Cyprus boninites and IAT) and O. Tsamerayn ($12\text{--}15^\circ\text{N}$ Mid-Atlantic Ridge MORB). D. Mangin provided technical help with the ion probe and the paper benefited from reviews by E. Deloule, M. Carrol, B. Scaillet, M. Pichavant and five anonymous reviewers. This study was supported by the International Science Foundation (MNN000), the Volkswagen Stiftung (I/68 569) and the Russian Basic Research Foundation (93-05-8895) through grants to A.V.S. This is CRPG-CNRS contribution 1137. [FA]

References

- [1] V.S. Sobolev, The constitution of the upper mantle and ways of magma generation, in: Vernadsky Readings, 40 pp., Moscow, 1973.

- [2] A.B. Thompson, Water in the Earth's mantle, *Nature* 358, 295–302, 1992.
- [3] D.R. Bell and G.R. Rossman, Water in the Earth's mantle: the role of nominally anhydrous minerals, *Science* 255, 1391–1397, 1992.
- [4] P.J. Michael, The concentration, behavior and storage of H₂O in the suboceanic upper mantle: implications for mantle metasomatism, *Geochim. Cosmochim. Acta* 52, 555–566, 1988.
- [5] J. Dixon, E. Stolper and J.R. Delaney, Infrared spectroscopic measurements of CO₂ and H₂O in Juan de Fuca Ridge basaltic glasses, *Earth Planet. Sci. Lett.* 90, 87–104, 1988.
- [6] A. Jambon and J.L. Zimmermann, Water in oceanic basalts: evidence for dehydration of recycled crust, *Earth Planet. Sci. Lett.* 101, 323–331, 1990.
- [7] J.G. Moore, Water content of basalt erupted on the ocean floor, *Contrib. Mineral. Petrol.* 28, 272–279, 1970.
- [8] D.W. Muenov, M.O. Garcia, K.E. Aggrey, U. Bednarz and H.U. Schminke, Volatiles in submarine glasses as a discriminant of tectonic origin: application to the Troodos ophiolite, *Nature* 343, 159–161, 1990.
- [9] C.D. Byers, M.O. Garcia and D.W. Muenov, Volatiles in basaltic glasses from the East Pacific Rise 21°N: implications for MORB sources and submarine lava flow morphology, *Earth Planet. Sci. Lett.* 79, 9–20, 1986.
- [10] J.R. Delaney, D.W. Muenov and D.G. Graham, Abundance and distribution of water, carbon and sulfur in the glassy rims of pillow basalts, *Geochim. Cosmochim. Acta* 48, 581–594, 1978.
- [11] F. Poreda, Helium-3 and deuterium in back arc basalts: Lau basin and the Mariana trough, *Earth Planet. Sci. Lett.* 73, 244–254, 1985.
- [12] L.V. Danyushevsky, T.J. Fallon, A.V. Sobolev, A.J. Crawford, M. Carrol and P.R. Price, The H₂O content of basalt glasses from South West Pacific back-arc basins, *Earth Planet. Sci. Lett.* 117, 347–362, 1993.
- [13] P.F. Dobson and J.R. O'Neil, Stable isotope compositions and water content of boninite series volcanic rocks from Chichi-jima, Bonin Islands, Japan, *Earth Planet. Sci. Lett.* 82, 75–86, 1987.
- [14] K.T. Kyser, W.E. Cameron and E.G. Nisbet, Boninite petrogenesis and alteration history: constraints from stable isotope composition of boninites from Cape Vogel, New Caledonia and Cyprus, *Contrib. Mineral. Petrol.* 93, 222–226, 1986.
- [15] K.T. Kyser and J.R. O'Neil, Hydrogen isotopes systematics of submarine basalts, *Geochim. Cosmochim. Acta* 48, 2123–2133, 1984.
- [16] D.H. Green, The origin of basaltic and nephelinitic magmas, *Trans. Leicester Lit. Philos. Soc.* 64, 28–54, 1970.
- [17] D.M. Harris and A.T.J. Anderson, Concentration, sources, and losses of H₂O, CO₂ and S in Kilauea basalt, *Geochim. Cosmochim. Acta* 47, 1139–1150, 1983.
- [18] D.M. Harris and A.T.J. Anderson, Volatiles H₂O, CO₂, and Cl in a subduction related basalt, *Contrib. Mineral. Petrol.* 87, 120–128, 1984.
- [19] R.N. Yanover, J.M. Sinton, M.A. Sommer and E.K. Gibson, C–O–H ratios in silicate melt inclusions in basalts from the Galapagos spreading center near 95°W: a laser decrepitation mass spectrometry study, *Geochim. Cosmochim. Acta* 53, 3145–3154, 1989.
- [20] T.W. Sisson and G.D. Layne, H₂O in basalt and basaltic andesite glass inclusions from four subduction-related volcanoes, *Earth Planet. Sci. Lett.* 117, 619–635, 1993.
- [21] S.J. Mackwell and D.L. Kohlstedt, Diffusion of hydrogen in olivine: implications for water in the mantle, *J. Geophys. Res.* 95, 5079–5088, 1990.
- [22] Z. Qin, F. Lu and A.T.J. Anderson, Diffusive reequilibration of melt and fluid inclusions, *Am. Mineral.* 77, 565–576, 1992.
- [23] E. Roedder, *Fluid Inclusions*, Rev. Mineral., 620 pp., 1984.
- [24] P.L. Roedder and R.F. Emslie, Olivine–liquid equilibrium, *Contrib. Mineral. Petrol.* 29, 275–289, 1970.
- [25] A.T. Anderson, Evidence for a picritic, volatile-rich magma beneath Mt. Shasta, California, *J. Petrol.* 15, 243–267, 1974.
- [26] T.J. Falloon and D.H. Green, Glass inclusions in magnesian olivine phenocrysts from Tonga: evidence for highly refractory parental magmas in the Tonga arc, *Earth Planet. Sci. Lett.* 81, 95–103, 1986.
- [27] A.V. Sobolev and L.V. Danyushevski, Petrology and geochemistry of boninites from the north termination of the Tonga trench: constraints on the generation conditions of primary high-Ca boninite magmas, *J. Petrol.* 35, 1183–1211, 1994.
- [28] A.V. Sobolev and N. Shimizu, Ultra-depleted primary melt included in an olivine from the Mid-Atlantic Ridge, *Nature* 363, 151–154, 1993.
- [29] E. Deloule, C. France-Lanord and F. Albarède, D/H analysis of minerals by ion probe, in: *Stable Isotope Geochemistry: A Tribute to Samuel Epstein*, H.P. Taylor, J.R. O'Neil and I.R. Kaplan, eds., pp. 53–62, *Geochem. Soc.*, 1991.
- [30] E. Stolper, Water in silicate glasses: an infrared spectroscopic study, *Contrib. Mineral. Petrol.* 81, 1–17, 1982.
- [31] E. Deloule, O. Paillat, M. Pichavant and B. Scaillet, Ion microprobe determination of water in silicate glasses: methods and applications, *Chem. Geol.* 125, 19–28, 1995.
- [32] A.B. Kersting and R.J. Arculus, Klyuchevskoy volcano, Kamchatka, Russia: the role of high-flux recharged, tapped and fractionated magma chamber(s) in the genesis of high Al₂O₃ from high MgO basalt, *J. Petrol.* 35, 1–41, 1994.
- [33] A.V. Sobolev et al., Petrology of ultramafic lavas and associated rocks of the Troodos massif, Cyprus, *Petrology* 1, 331–361, 1993.
- [34] D.A. Walker and W.E. Cameron, Boninite primary magmas: evidence from the Cape Vogel peninsula, PNG, *Contrib. Mineral. Petrol.* 83, 150–158, 1983.
- [35] S. Newman and S. van der Laan, Volatile contents of Izu–Bonin forearc volcanic glasses, *Proc. ODP, Sci. Results* 125, 131–139, 1992.
- [36] H.S. Smith and A.J. Erlank, Geochemistry and petrogenesis of komatiites from the Barberton greenstone belt, South Africa, in: *Komatiites*, N.T. Arndt and E.G. Nisbet, eds., pp. 347–397, Allen and Unwin, London, 1982.

- [37] T.W. Sisson and T.L. Grove, Temperatures and H₂O contents of low-MgO high-alumina basalts, *Contrib. Mineral. Petrol.* 113, 167–184, 1993.
- [38] C.E. Ford, D.G. Russel, J.A. Groven and M.R. Fisk, Distribution coefficients of Mg²⁺, Fe²⁺, Ca²⁺ and Mn²⁺ between olivine and melt, *J. Petrol.* 24, 256–265, 1983.
- [39] P. Michael, Regionally distinctive source of depleted MORB: evidence for trace elements and H₂O, *Earth Planet. Sci. Lett.* 131, 301–320, 1995.
- [40] Q. Bai and D.L. Kohlstedt, Substantial hydrogen solubility in olivine and implications for water storage in the mantle, *Nature* 357, 672–674, 1992.
- [41] A.R. Pawley and J.R. Holloway, Water sources for subduction zone volcanism: new experimental constraints, *Science* 260, 664–667, 1993.
- [42] A.J. Crawford, T.J. Falloon and D.H. Green, Classification, petrogenesis and tectonic setting of boninites, in: *Boninites and Related Rocks*, A.J. Crawford, ed., pp. 1–49, Unwin Hyman, London, 1989.
- [43] F. Albarède, How deep do common basaltic magmas form and differentiate?, *J. Geophys. Res.* 97, 10997–11009, 1992.
- [44] G. Thompson, Basalt–seawater interaction, in: *Hydrothermal Processes at Seafloor Spreading Centers*, P.A. Rona, K. Boström, L. Laubier and K.L.J. Smith, eds., pp. 225–278, Plenum, New York, 1983.
- [45] E. Stolper and S. Newman, The role of water in the petrogenesis of Mariana trough basalts, *Earth Planet. Sci. Lett.* 121, 293–325, 1994.
- [46] M.E. Schneider and D.H. Eggler, Fluids in equilibrium with peridotite minerals: implications for mantle metasomatism, *Geochim. Cosmochim. Acta* 50, 711–724, 1986.
- [47] E. Deloule, F. Albarède and S.M.F. Sheppard, Hydrogen isotope heterogeneities in the mantle from ion probe analysis of amphiboles from ultramafic rocks, *Earth Planet. Sci. Lett.* 105, 543–553, 1991.
- [48] S.M. Peacock, Fluid processes in subduction zones, *Science* 248, 329–337, 1990.
- [49] T. Staudacher and C.J. Allègre, Recycling of oceanic crust and sediments: the noble gas subduction barrier, *Earth Planet. Sci. Lett.* 89, 173–183, 1988.